

Optimal SNR Analysis for Single-user RIS Systems

Ikram Singh*, Peter J. Smith†, Pawel A. Dmochowski*

*School of Engineering and Computer Science, Victoria University of Wellington, Wellington, New Zealand

†School of Mathematics and Statistics, Victoria University of Wellington, Wellington, New Zealand

email: {ikram.singh,peter.smith,pawel.dmochowski}@ecs.vuw.ac.nz

Abstract—In this paper, we present an analysis of the optimal uplink SNR of a SIMO Reconfigurable Intelligent Surface (RIS)-aided wireless link. We assume that the channel between base station and RIS is a rank-1 LOS channel while the user (UE)-RIS and UE-base station (BS) channels are correlated Rayleigh. We derive an exact closed form expression for the mean SNR and an approximation for the SNR variance leading to an accurate gamma approximation to the distribution of the UL SNR. Furthermore, we analytically characterise the effects of correlation on SNR, showing that correlation in the UE-BS channel can have negative effects on the mean SNR, while correlation in the UE-RIS channel improves system performance. For systems with a large number of RIS elements, correlation in the UE-RIS channel can cause an increase in the mean SNR of up to 27.32% relative to an uncorrelated channel.

I. INTRODUCTION

Reconfigurable Intelligent Surface (RIS) aided wireless networks are currently the subject of considerable research attention due to their ability to manipulate the channel between users (UEs) and base station (BS) via the RIS. Assuming that channel state information (CSI) is known at the RIS, one can intelligently alter the RIS phases, essentially changing the channel, to improve various aspects of system performance. Here, we focus on a single user system and assume that the RIS is carefully located near the BS such that a rank-1 line-of-sight (LOS) channel is formed between the BS and RIS.

System scenarios with a LOS channel between the BS-RIS and a single-user are also considered in [1]–[3] with motivation for the LOS assumption given in [2]. All of these existing works aim to enhance the system to achieve some optimal system performance (e.g. sum rate, SINR, etc.) by tuning the RIS phases. In particular, [3] and [2] provide a closed form RIS phase solution with and without the presence of a direct UE-BS channel for a single user setting, respectively. However, once the optimal RIS has been defined there is no *exact* analysis of the mean SNR and no analysis of correlation impact on the mean SNR in [1]–[3].

For the UE to RIS and the direct UE to BS links, scattered channels are a reasonable assumption and spatial correlation in the channels is an important factor, especially at the RIS where small inter-element spacing may be envisaged. Several papers do consider spatial correlation in the small-scale fading channels [2], [4]–[8], however, these papers are simulation based and no *exact* analysis is given on the impact of correlation on the mean SNR.

Statistical properties of the channel have been investigated in existing literature. For example, [9], [10] provide a closed

form expression for the mean SNR in the absence of a UE-BS channel with [10] additionally providing a probability density function (PDF) and a cumulative distribution function (CDF) for the distribution of the SNR. In [9], [11], an upper bound is given for the ergodic capacity and in [12] a lower bound is given for the ergodic capacity. However, there is no existing literature on closed form expressions for the mean SNR and SNR variance of an optimal RIS-aided wireless system, in the presence of correlated UE-BS, UE-RIS fading channels.

Hence, in this paper, we focus on an analysis of the optimal uplink (UL) SNR for a single user RIS aided link with a rank-1 LOS RIS-BS channel and correlated Rayleigh fading for the UE-BS and UE-RIS channels¹. In particular, for this system and channel model we make the following contributions:

- An exact closed-form result for mean SNR and an approximate closed form expression for SNR variance are derived. We show that a gamma distribution provides a good approximation of the UL optimal SNR distribution.
- Exact closed-form expressions for both mean SNR and SNR variance are derived for uncorrelated Rayleigh channels and presented as a special case.
- The analysis is leveraged to gain insight into the impact of spatial correlation and system dimension on the mean SNR. We prove that correlation in the UE-BS channel can have negative effects, while correlation in the UE-RIS channel improves the mean SNR. For systems with a large number of RIS elements, the latter improvement saturates to a relative gain of approximately 27.32%.

Notation: $\mathbb{E}\{\cdot\}$ represents statistical expectation. $\Re\{\cdot\}$ is the Real operator. $\|\cdot\|_2$ denotes the ℓ_2 norm. $\mathcal{CN}(\mu, \mathbf{Q})$ denotes a complex Gaussian distribution with mean μ and covariance matrix \mathbf{Q} . $\mathbf{1}_n$ represents an $n \times n$ matrix with unit entries. The transpose, Hermitian transpose and complex conjugate operators are denoted as $(\cdot)^T, (\cdot)^H, (\cdot)^*$, respectively. The angle of a vector \mathbf{x} of length N is defined as $\angle \mathbf{x} = [\angle x_1, \dots, \angle x_N]^T$ and the exponent of a vector is defined as $e^{\mathbf{x}} = [e^{x_1}, \dots, e^{x_N}]^T$.

II. SYSTEM MODEL

As shown in Fig. 1, we examine a RIS aided single user single input multiple output (SIMO) system where a RIS with N reflective elements is located close to a BS with M antennas such that a rank-1 LOS condition is achieved between the RIS and BS.

¹An extension to this work is being developed which considers Ricean fading for the UE-BS and UE-RIS channels.

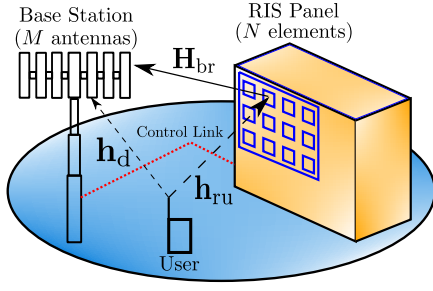


Fig. 1: System model.

A. Channel Model

Let $\mathbf{h}_d \in \mathbb{C}^{M \times 1}$, $\mathbf{h}_{ru} \in \mathbb{C}^{N \times 1}$, $\mathbf{H}_{br} \in \mathbb{C}^{M \times N}$ be the UE-BS, UE-RIS and RIS-BS channels, respectively. The diagonal matrix $\Phi \in \mathbb{C}^{N \times N}$, where $\Phi_{r,r} = e^{j\phi_r}$ for $r = 1, 2, \dots, N$, contains the reflection coefficients for each RIS element. The global UL channel is thus represented by

$$\mathbf{h} = \mathbf{h}_d + \mathbf{H}_{br} \Phi \mathbf{h}_{ru}. \quad (1)$$

In the channel model, we consider the correlated Rayleigh channels: $\mathbf{h}_d = \sqrt{\beta_d} \mathbf{R}_d^{1/2} \mathbf{u}_d$ and $\mathbf{h}_{ru} = \sqrt{\beta_{ru}} \mathbf{R}_{ru}^{1/2} \mathbf{u}_{ru} \triangleq \sqrt{\beta_{ru}} \tilde{\mathbf{h}}_{ru}$ where β_d and β_{ru} are the link gains, \mathbf{R}_d and \mathbf{R}_{ru} are the correlation matrices for UE-BS and UE-RIS links respectively and $\mathbf{u}_d, \mathbf{u}_{ru} \sim \mathcal{CN}(\mathbf{0}, \mathbf{I})$. The rank-1 LOS channel from RIS to BS has link gain β_{br} and is given by $\mathbf{H}_{br} = \sqrt{\beta_{br}} \mathbf{a}_b \mathbf{a}_r^H$ where \mathbf{a}_b and \mathbf{a}_r are topology specific steering vectors at the BS and RIS respectively. Particular examples of steering vectors for a vertical uniform rectangular array (VURA) are in Sec. V.

Note, that the correlation matrices \mathbf{R}_{ru} and \mathbf{R}_d can represent any correlation model. For simulation purposes, we will use the well-known exponential decay model,

$$(\mathbf{R}_{ru})_{ik} = \rho_{ru} \frac{d_{i,k}}{d_r^{2\alpha}}, \quad (\mathbf{R}_d)_{ik} = \rho_d \frac{d_{i,k}}{d_b^{2\alpha}}, \quad (2)$$

where $0 \leq \rho_{ru} \leq 1$, $0 \leq \rho_d \leq 1$. $d_{i,k}$ is the distance between the i^{th} and k^{th} antenna/element at the BS/RIS. d_b and d_r are the nearest-neighbour BS antenna separation and RIS element separation, respectively, which are measured in wavelength units. ρ_d and ρ_{ru} are the nearest neighbour BS antenna and RIS element correlations, respectively.

B. Optimal SNR

Using (1), the received signal at the BS is, $\mathbf{r} = (\mathbf{h}_d + \mathbf{H}_{br} \Phi \mathbf{h}_{ru}) s + \mathbf{n} \triangleq \mathbf{h} s + \mathbf{n}$, where s is the transmitted signal with power E_s and $\mathbf{n} \sim \mathcal{CN}(\mathbf{0}, \sigma^2 \mathbf{I})$. For a single user system, matched filtering (MF) is the optimal combining method, with UL SNR, given by $\text{SNR} = \mathbf{h}^H \mathbf{h} \bar{\tau}$, where $\bar{\tau} = \frac{E_s}{\sigma^2}$. The optimal RIS phase matrix to maximize the SNR can be computed using the main steps outlined in [3, Sec. III-B] but using an UL channel model instead of downlink. Substituting the channel vectors and through some algebraic manipulation, the optimal RIS phase matrix is

$$\Phi = \frac{\mathbf{a}_b^H \mathbf{h}_d}{|\mathbf{a}_b^H \mathbf{h}_d|} \text{diag}\{e^{j\angle \mathbf{a}_r}\} \text{diag}\{e^{-j\angle \mathbf{h}_{ru}}\}. \quad (3)$$

Substituting (3) into \mathbf{h} , the optimal UL global channel is,

$$\mathbf{h} = \mathbf{h}_d + \sqrt{\beta_{br} \beta_{ru}} \psi \sum_{n=1}^N \left| \tilde{\mathbf{h}}_{ru,n} \right| \mathbf{a}_b, \quad (4)$$

where $\psi = \mathbf{a}_b^H \mathbf{h}_d / |\mathbf{a}_b^H \mathbf{h}_d|$. Hence, the optimal UL SNR is

$$\text{SNR} = (\mathbf{h}_d^H + \alpha^* \mathbf{a}_b^H) (\mathbf{h}_d + \alpha \mathbf{a}_b) \bar{\tau}, \quad (5)$$

where $\alpha = \sqrt{\beta_{br} \beta_{ru}} \psi \sum_{n=1}^N \left| \tilde{\mathbf{h}}_{ru,n} \right| \triangleq \sqrt{\beta_{br} \beta_{ru}} \psi Y$.

III. $\mathbb{E}\{\text{SNR}\}$ AND $\text{VAR}\{\text{SNR}\}$

A. Correlated Rayleigh Case

Here, we provide an exact closed form result for $\mathbb{E}\{\text{SNR}\}$ and an exact expression for $\text{Var}\{\text{SNR}\}$.

Theorem 1. The mean SNR is given by

$$\mathbb{E}\{\text{SNR}\} = \left(\beta_d M + \frac{N A \pi \sqrt{\beta_d \beta_{br} \beta_{ru}}}{2} + \beta_{br} \beta_{ru} M(N+F) \right) \bar{\tau}, \quad (6)$$

with F given by

$$F = \sum_{i=1}^N \sum_{\substack{j=1 \\ i \neq j}}^N \frac{\pi}{4} \left(1 - |\rho_{ij}|^2 \right)^2 {}_2F_1 \left(\frac{3}{2}, \frac{3}{2}; 1; |\rho_{ij}|^2 \right), \quad (7)$$

and $A = \left\| \mathbf{R}_d^{1/2} \mathbf{a}_b \right\|_2$, where ${}_2F_1(\cdot)$ is the Gaussian hypergeometric function and $\rho_{ij} = (\mathbf{R}_{ru})_{ij}$.

Proof. See App. A for the derivation of (6). ■

Theorem 2. The SNR variance is given by

$$\begin{aligned} \text{Var}\{\text{SNR}\} = & \left(\beta_d^2 \text{tr}\{\mathbf{R}_d\} + \beta_d^{3/2} \sqrt{\beta_{br} \beta_{ru}} N \pi (B - MA) \right. \\ & + \beta_d \beta_{br} \beta_{ru} A^2 \left(4(N+F) - \frac{N^2 \pi^2}{4} \right) \\ & + MA \sqrt{\beta_d} (\beta_{br} \beta_{ru})^{3/2} (2\sqrt{\pi} C_1 - N(N+F)\pi) \\ & \left. + (M \beta_{br} \beta_{ru})^2 (C_2 - (N+F)^2) \right) \bar{\tau}^2, \quad (8) \end{aligned}$$

where $B = MA + \mathbf{a}_b^H \mathbf{R}_d \mathbf{a}_b / 2A$, F is given by (7), A is given in Theorem 1 and $C_1 = \mathbb{E}\{Y^3\}$, $C_2 = \mathbb{E}\{Y^4\}$.

Proof. See App. B for the derivation of (8). ■

In (8), all terms are known except for C_1 and C_2 , the third and fourth moments of Y . To the best of our knowledge, these moments are intractable so we present approximations of C_1 and C_2 in the following Corollary.

Corollary 1. To obtain an SNR variance approximation in closed form, we approximate the 3rd, 4th moments of Y by,

$$\mathbb{E}\{Y^3\} = b^3 a \prod_{k=1}^2 (k+a), \quad \mathbb{E}\{Y^4\} = b^4 a \prod_{k=1}^3 (k+a) \quad (9)$$

with

$$a = \frac{N^2 \pi}{4(N+F) - N^2 \pi}, \quad b = \frac{2}{N \sqrt{\pi}} \left(N+F - \frac{N^2 \pi}{4} \right).$$

where F is given by (7).

Proof. See App. C for the derivation of (9). ■

From Theorem 1 and the Corollary, we have $\mathbb{E}\{\text{SNR}\}$ and an approximation to $\text{Var}\{\text{SNR}\}$. This enable us to fit a gamma

distribution as an approximation to the SNR distribution. Motivation and reasoning for this approach is given in Sec. V-A.

B. Special Case: Uncorrelated Rayleigh Case

For independent Rayleigh fading, we provide exact closed form expressions for both $\mathbb{E}\{\text{SNR}\}$ and $\text{Var}\{\text{SNR}\}$. Here, $\mathbf{h}_d, \mathbf{h}_{ru} \sim \mathcal{CN}(\mathbf{0}, \mathbf{I})$ and as such, (7) simplifies to

$$F_u = \sum_{i=1}^N \sum_{\substack{j=1 \\ i \neq j}}^N \frac{\pi}{4} = N(N-1) \frac{\pi}{4}. \quad (10)$$

From $\|\mathbf{a}_b\|_2 = \sqrt{M}$, the value of $\mathbb{E}\{\text{SNR}\}$ is,

$$\left(\beta_d M + \frac{\sqrt{M} N \pi}{2} \sqrt{\beta_d \beta_{br} \beta_{ru}} + \beta_{br} \beta_{ru} M (N + F_u) \right) \bar{\tau}. \quad (11)$$

Using (10), an exact expression for $\text{Var}\{\text{SNR}\}$ is given by

$$\begin{aligned} & \left(\beta_d^2 M + \beta_d^{3/2} \sqrt{\beta_{br} \beta_{ru}} N \pi (B_u - 2M^{3/2}) \right. \\ & \left. + \beta_d \beta_{br} \beta_{ru} M \left(4(N + F_u) - \frac{N^2 \pi^2}{4} \right) \right. \\ & \left. + M^{3/2} \sqrt{\beta_d} (\beta_{br} \beta_{ru})^{3/2} (2\sqrt{\pi} C_{u1} - N(N + F_u) \pi) \right. \\ & \left. + (M \beta_{br} \beta_{ru})^2 (C_{u2} - (N + F_u)^2) \right) \bar{\tau}^2, \end{aligned} \quad (12)$$

with

$$B_u = M^{3/2} + \frac{\sqrt{M}}{2}, \quad C_{u1} = \frac{N\sqrt{\pi}}{2} \left(\frac{\pi}{4} \prod_{k=1}^2 (N-k) + 3N - \frac{3}{2} \right)$$

$$C_{u2} = 2N + \binom{N}{2} \left(\prod_{k=2}^3 (N-k) \frac{\pi^2}{8} + 6 + 3\pi(N-1) \right)$$

where F_u is given by (10). Derivations for C_{u1} , C_{u2} are omitted for reasons of space, but can be easily obtained by expanding Y^3 , Y^4 and computing the expectation of each term using the following: $\mathbb{E}\left\{|\tilde{\mathbf{h}}_{ru,i}|^4\right\} = 2$, $\mathbb{E}\left\{|\tilde{\mathbf{h}}_{ru,i}|^3\right\} = 3\sqrt{\pi}/4$, $\mathbb{E}\left\{|\tilde{\mathbf{h}}_{ru,i}|^2\right\} = 1$, $\mathbb{E}\left\{|\tilde{\mathbf{h}}_{ru,i}|\right\} = \sqrt{\pi}/2$.

IV. PERFORMANCE INSIGHTS BASED ON $\mathbb{E}\{\text{SNR}\}$

Correlation in \mathbf{h}_d and \mathbf{h}_{ru} have separable effects on the mean SNR in (6). Specifically, the second term in (6) is only affected by ρ_d and the third term is only affected by ρ_{ru} whilst the first term is affected by neither. Here, we present an analysis of $\mathbb{E}\{\text{SNR}\}$ with respect to the correlations ρ_{ru}, ρ_d and give asymptotic results for large N .

A. Effect of ρ_{ru} on $\mathbb{E}\{\text{SNR}\}$

With respect to the correlation level ρ_{ru} , (6) can be lower and upper bounded due to F being monotonic in ρ_{ru} [13, Eq. (15.1.1)]. The upper bound for (7) as $\rho_{ru} \rightarrow 1$ is

$$F_{\text{UB}} \stackrel{(a)}{=} \sum_{i=1}^N \sum_{\substack{j=1 \\ i \neq j}}^N \frac{\pi}{4} {}_2F_1 \left(-\frac{1}{2}, -\frac{1}{2}; 1; 1 \right) \stackrel{(b)}{=} N(N-1), \quad (13)$$

where (a) uses [13, Eq. (15.3.3)] to perform a linear transformation of the hypergeometric function and (b) uses [13, Eq. (15.1.20)] to reduce the hypergeometric function to a known

value along with evaluation of the double summation. Using (10) and (13), (7) has the following upper and lower bounds,

$$F_u = N(N-1) \frac{\pi}{4} \leq F \leq N(N-1). \quad (14)$$

Hence the upper and lower bounds for SNR w.r.t. ρ_{ru} are

$$\mathbb{E}\{\text{SNR}\}_{\text{UB}} = \left(\beta_d M + \frac{NA\pi}{2} \sqrt{\beta_d \beta_{br} \beta_{ru}} + \beta_{br} \beta_{ru} MN^2 \right) \bar{\tau}, \quad (15)$$

$$\mathbb{E}\{\text{SNR}\}_{\text{LB}} =$$

$$\left(\beta_d M + \frac{NA\pi}{2} \sqrt{\beta_d \beta_{br} \beta_{ru}} + \beta_{br} \beta_{ru} M(N + F_u) \right) \bar{\tau}. \quad (16)$$

We observe that correlation in \mathbf{h}_{ru} improves the mean SNR. From (15) and (16) we observe that the first term in $\mathbb{E}\{\text{SNR}\}$ is of order M and the third term is of order MN^2 . In Sec. IV-B we show that the second term has a maximum order of MN . Hence, the third term is dominant giving $\mathbb{E}\{\text{SNR}\} = \mathcal{O}(MN^2)$ and the largest channel effect will be an increase in SNR due to correlation at the RIS.

B. Effect of ρ_d on $\mathbb{E}\{\text{SNR}\}$

The only variable in (6) that is affected by ρ_d is A . As $\rho_d \rightarrow 0$, $A \rightarrow \sqrt{M}$. As $\rho_d \rightarrow 1$, $\mathbf{R}_d \rightarrow \mathbf{1}_M$ which means that

$$A = \left\| \mathbf{R}_d^{1/2} \mathbf{a}_b \right\|_2 \rightarrow \frac{1}{\sqrt{M}} \left\| \mathbf{1}_M \mathbf{a}_b \right\|_2 = \left| \sum_{i=1}^M \mathbf{a}_{b,i} \right| \leq M.$$

Hence, the second term in (6) has a maximum order of MN as stated above. Although the maximum order can be achieved with perfect correlation ($\rho_d = 1$), for typical environments the value of A tends to reduce as correlation is increased. To explain this property we show via an example based on a uniform linear array (ULA) that for highly correlated BS antennas, \sqrt{M} tends to be larger than $\left| \sum_{i=1}^M \mathbf{a}_{b,i} \right|$ for large M . For a ULA, ignoring elevation angles, the steering vector elements can be given by $\mathbf{a}_{b,i} = e^{j2\pi(i-1)d_b \sin(\theta)}$ where θ is the azimuth angle of arrival at the BS. Here,

$$\left| \sum_{i=1}^M \mathbf{a}_{b,i} \right| = \left| \frac{1 - e^{j2M\pi d_b \sin(\theta)}}{1 - e^{j2\pi d_b \sin(\theta)}} \right| = \left| \frac{\sin(M\pi d_b \sin(\theta))}{\sin(\pi d_b \sin(\theta))} \right|.$$

This well-known sinusoidal ratio is much smaller than \sqrt{M} for large M and as long as θ is not arbitrarily close to zero. Therefore, systems with a large number of BS antennas can expect greater system performance when \mathbf{h}_d is uncorrelated unless the RIS-BS link is extremely close to broadside.

In summary, high correlation at the RIS and low correlation at the BS tend to be beneficial. We refer to this scenario as the *favorable channel scenario*.

C. Favorable Channel Scenario and Asymptotic Analysis

Using the analysis in Sec. IV-A and Sec. IV-B, the favorable channel scenario is given by: $\mathbf{h}_{ru} \sim \mathcal{CN}(\mathbf{0}, \mathbf{1}_N)$, $\mathbf{h}_d \sim \mathcal{CN}(\mathbf{0}, \mathbf{I}_M)$. The resulting mean SNR is obtained by substituting the UB of (14) and $A = \sqrt{M}$ into (6), giving

$$\mathbb{E}\{\text{SNR}_{\text{fav}}\} = \left(\beta_d M + \frac{N\sqrt{M}\pi}{2} \sqrt{\beta_d \beta_{br} \beta_{ru}} + \beta_{br} \beta_{ru} MN^2 \right) \bar{\tau}. \quad (17)$$

Next, we consider the asymptotic gains achievable through increased correlation at the RIS. The relative gain due to correlation can be defined as

$$\text{Gain}_{\text{corr}} = \frac{\mathbb{E}\{\text{SNR}\}_{\text{UB}} - \mathbb{E}\{\text{SNR}\}_{\text{LB}}}{\mathbb{E}\{\text{SNR}\}_{\text{LB}}} \quad (18)$$

$$\stackrel{(a)}{=} \frac{(4 - \pi)N^2 + (\pi - 4)N}{\pi N^2 + (4 - \pi)N + \frac{4\beta_d}{\beta_{\text{br}}\beta_{\text{ru}}} + \frac{2NA\pi\sqrt{\beta_d}}{M\sqrt{(\beta_{\text{br}}\beta_{\text{ru}})}}}$$

where (a) involves substituting (15) and (16) and performing simple algebraic manipulations. Therefore, as $N \rightarrow \infty$,

$$\text{Gain}_{\text{max}} = \lim_{N \rightarrow \infty} \text{Gain}_{\text{corr}} = \frac{4 - \pi}{\pi} \approx 27.32\%.$$

Hence, for a large RIS, the maximum gain due to correlation in the UE-RIS Rayleigh channel is approximately 27.32%. Also, observe that negative effects on the mean SNR due to correlation in the direct channel are minimized as N increases.

V. RESULTS

We present numerical results to verify the analysis in Secs. III and IV. We do not consider cell-wide averaging as the focus is on the SNR distribution over the fast fading. Furthermore, the relationship between the SNR and the gains, $\beta_d, \beta_{\text{br}}$ and β_{ru} , is straightforward, as shown in (6). Hence, we present numerical results for fixed link gains. In particular, as the RIS-BS link is LOS we assume $\beta_{\text{br}} = d_{\text{br}}^{-2}$ where $d_{\text{br}} = 20\text{m}$. Next, for simplicity, $\beta_d = \beta_{\text{ru}} = 0.59$. This was chosen to give the 95%-ile of the SNR distribution as 25 dB in the baseline case of moderate channel correlation (see $\rho_d = \rho_{\text{ru}} = 0.7$ in Fig. 2), with $M = 32, N = 64$.

As stated in Sec. II-A, the steering vectors for \mathbf{H}_{br} are not restricted to any particular formation. However, for simulation purposes, we will use the VURA model as outlined in [14], but in the $y-z$ plane with equal spacing in both dimensions at both the RIS and BS. The y, z components of the steering vector at the BS are $\mathbf{a}_{\text{b},y}$ and $\mathbf{a}_{\text{b},z}$ which are given by

$$[1, e^{j2\pi d_b \sin(\theta_A) \sin(\omega_A)}, \dots, e^{j2\pi d_b (M_y - 1) \sin(\theta_A) \sin(\omega_A)}]^T,$$

$$[1, e^{j2\pi d_b \cos(\theta_A)}, \dots, e^{j2\pi d_b (M_z - 1) \cos(\theta_A)}]^T,$$

respectively. Similarly at the RIS, $\mathbf{a}_{\text{r},y}$ and $\mathbf{a}_{\text{r},z}$ are defined by,

$$[1, e^{j2\pi d_r \sin(\theta_D) \sin(\omega_D)}, \dots, e^{j2\pi d_r (N_y - 1) \sin(\theta_D) \sin(\omega_D)}]^T,$$

$$[1, e^{j2\pi d_r \cos(\theta_D)}, \dots, e^{j2\pi d_r (N_z - 1) \cos(\theta_D)}]^T,$$

respectively where $M = M_y M_z, N = N_y N_z, d_b = 0.5, d_r = 0.2$, where d_b and d_r are in wavelength units. Therefore, the steering vectors at the BS and RIS are then given by,

$$\mathbf{a}_{\text{b}} = \mathbf{a}_{\text{b},y} \otimes \mathbf{a}_{\text{b},z}, \quad \mathbf{a}_{\text{r}} = \mathbf{a}_{\text{r},y} \otimes \mathbf{a}_{\text{r},z}, \quad (19)$$

respectively, where \otimes denotes the Kronecker product, θ_A and ω_A are elevation/azimuth angles of arrival (AOAs) at the BS and θ_D, ω_D are the corresponding angles of departure (AODs) at the RIS. The elevation/azimuth angles are selected based on the following geometry representing a range of LOS \mathbf{H}_{br} links with less elevation variation than azimuth variation: $\theta_D \sim \mathcal{U}[70^\circ, 90^\circ], \omega_D \sim \mathcal{U}[-30^\circ, 30^\circ], \theta_A = 180^\circ - \theta_D, \omega_A \sim \mathcal{U}[-30^\circ, 30^\circ]$ where $\mathcal{U}[a, b]$ denotes a uniform random variable taking on values between a and b . For all results in this paper we use a single sample from this

range of angles given by $\theta_D = 77.1^\circ, \omega_D = 19.95^\circ, \theta_A = 109.9^\circ, \omega_A = -29.9^\circ$. Note that all of these parameter values and variable definitions are not altered throughout the results and figures, unless specified otherwise.

A. Approximate CDF for SNR

It is known that the SNR of a wide range of fading channels can be approximated by a mixture gamma distribution [15]. Also, it is well-known that a single gamma approximation is often reasonable for a sum of a number of positive random variables [9]. Motivated by this, we approximate the SNR in (5) by a single gamma variable.

The shape parameter of a gamma approximation to the SNR is given by $k_\gamma = \frac{\mathbb{E}\{\text{SNR}\}^2}{\text{Var}\{\text{SNR}\}}$ and the scale parameter is $\theta_\gamma = \frac{\text{Var}\{\text{SNR}\}}{\mathbb{E}\{\text{SNR}\}}$ where $\mathbb{E}\{\text{SNR}\}$ and $\text{Var}\{\text{SNR}\}$ are given in Sec. III. Using these values of k_γ, θ_γ , the analytical and simulated SNR CDFs are shown in Fig. 2 for $N = 64$ and $N = 256$, both with $\rho_{\text{ru}} = \rho_d \in \{0, 0.7, 0.95\}$. When computing the analytical SNR CDFs, for $\rho_{\text{ru}} = \rho_d = 0$, (11) and (12) were used and for $\rho_{\text{ru}} = \rho_d \neq 0$, (6) and (8) were used. As expected, there is a very good agreement between the

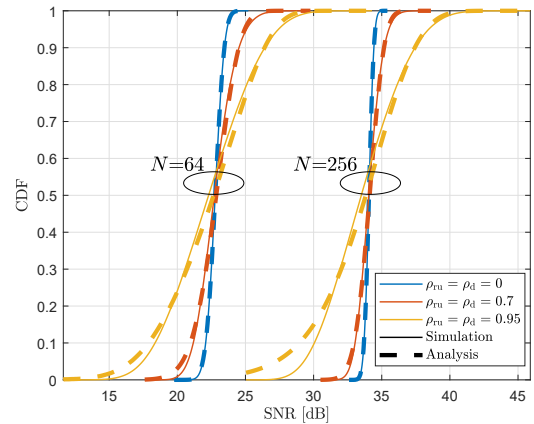


Fig. 2: Simulated and analytical CDFs for $N = 64$ and $N = 256$, both with $\rho_{\text{ru}} = \rho_d = \{0, 0.7, 0.95\}$

simulated and analytical SNR CDFs when $\rho_d = \rho_{\text{ru}} = 0$ due to exact mean SNR and SNR variance expressions. Increasing the correlation level causes the CDF agreement to deviate slightly in the low SNR region, especially in the highest correlation scenario. Good agreement is maintained in the mid-high SNR region. The gamma distribution therefore provides a good representation of the UL SNR unless the correlations become very high.

B. ρ_d, ρ_{ru} and Asymptotic Analysis Results

Here, we verify the performance insights based on $\mathbb{E}\{\text{SNR}\}$. Fig. 3 represents SNR simulations and analysis for three different correlation scenarios: $\rho_{\text{ru}} = \rho_d = 0, \rho_{\text{ru}} = \rho_d = 1$ and the favorable channel scenario $\rho_{\text{ru}} = 1, \rho_d = 0$. The left subfigure in Fig. 3 shows the quadratic increase in mean SNR, as predicted by the analysis. The favorable channel scenario yields the highest mean SNR, but the increase over perfect correlation in both channels is marginal. The lowest

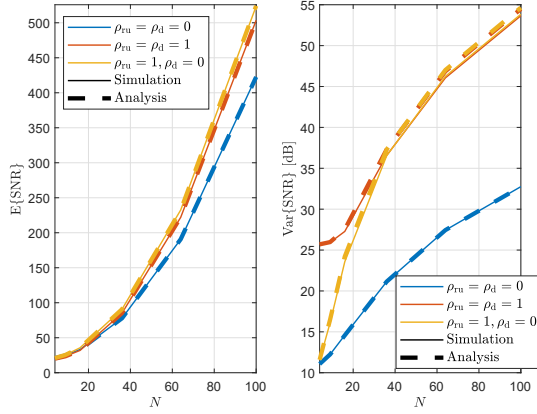


Fig. 3: Simulated and analytical mean and variance results for SNR with three different correlation scenarios: $\rho_{ru} = \rho_d = 0$, $\rho_{ru} = \rho_d = 1$ and favorable channel scenario $\rho_{ru} = 1, \rho_d = 0$.

SNR occurs when both channels are uncorrelated. Fig. 3 also shows that for all correlation scenarios, the theoretical analysis agrees with simulations.

The right subfigure in Fig. 3 shows the accuracy of the SNR variance approximation. There is a perfect agreement for the case where \mathbf{h}_{ru} and \mathbf{h}_d are uncorrelated. In the correlated cases, the analysis and simulation agree closely for low N but begin to deviate slightly as N grows. This is also reflected in Fig. 2 as the CDF agreement between simulation and analysis is worse for $N = 256$ compared to $N = 64$ as $\rho_d, \rho_{ru} \rightarrow 1$. Note that the analytical CDFs show a longer lower tail, partially caused by the over-estimate of the variance. As N grows, observe that the variance for scenarios $\rho_{ru} = \rho_d = 1$ and $\rho_{ru} = 1, \rho_d = 0$ converge to approximately the same value since the effects of correlation in \mathbf{h}_d are reduced by large N .

Finally, in Fig. 4 we verify the mean SNR relative gain due to correlation in \mathbf{h}_{ru} , and verify the asymptotic analysis in Sec. IV-A and Sec. IV-C. For simplicity, we assume all three channels have the same link gain and let $\beta_d = \beta_{ru} = \beta_{br} = 1$. Fig. 4 verifies the analysis in Sec. IV-C demonstrating an

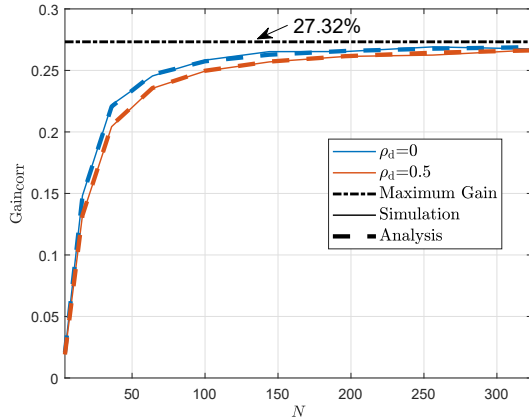


Fig. 4: Average SNR gain due to correlation in \mathbf{h}_{ru} for varying RIS sizes and correlation in \mathbf{h}_d .

increasing gain with correlation saturating at approximately 27.32%. Introducing correlation in the direct channel causes

the gain to be lower. However, as explained in the analysis, for large RIS elements, this negative effect is reduced.

VI. CONCLUSION

We derive an exact closed form expression for the mean SNR of the optimal single user RIS design where spatially correlated Rayleigh fading is assumed for the UE-BS and UE-RIS channels and the RIS-BS channel is LOS. We also provide an accurate approximation to the SNR variance and a gamma approximation to the CDF of the SNR. The results offers new insight into how spatial correlation impacts the mean SNR and scenarios in which we would expect high SNR performance.

APPENDIX A

$\mathbb{E}\{\text{SNR}\}$ DERIVATION IN SEC. III-A

Substituting the channel vectors and matrices described in Sec. II-A into (5) gives

$$\text{SNR} = \left(\beta_d \mathbf{u}_d^H \mathbf{R}_d \mathbf{u}_d + 2\sqrt{\beta_d} \Re \left\{ \alpha \mathbf{u}_d^H \mathbf{R}_d^{1/2} \mathbf{a}_b \right\} + |\alpha|^2 M \right) \bar{\tau} \triangleq (S_1 + S_2 + S_3) \bar{\tau}.$$

We compute $\mathbb{E}\{\text{SNR}\}$ by taking the expectation of each term.

Term 1: Since $\mathbf{u}_d \sim \mathcal{CN}(\mathbf{0}, \mathbf{I})$,

$$\mathbb{E}\{S_1\} = \beta_d \text{tr}\{\mathbf{R}_d\} = \beta_d M. \quad (20)$$

Term 2: Substituting α from Sec. II-B we have,

$$\mathbb{E}\{S_2\} = 2\sqrt{\beta_d \beta_{br} \beta_{ru}} \mathbb{E}\{Y\} \mathbb{E}\left\{ \left| \mathbf{a}_b^H \mathbf{R}_d^{1/2} \mathbf{u}_d \right| \right\}.$$

Since $\mathbf{h}_{ru} \sim \mathcal{CN}(\mathbf{0}, \mathbf{R}_{ru})$ it follows that $\mathbb{E}\{Y\} = \frac{N\sqrt{\pi}}{2}$ [16]. To compute $\mathbb{E}\left\{ \left| \mathbf{a}_b^H \mathbf{R}_d^{1/2} \mathbf{u}_d \right| \right\}$, note the following results. As $\mathbf{u}_d \sim \mathcal{CN}(\mathbf{0}, \mathbf{I}_M)$, it follows that $\mathbf{a}_b^H \mathbf{R}_d^{1/2} \mathbf{u}_d$ is zero mean complex Gaussian with $\mathbb{E}\left\{ \left| \mathbf{a}_b^H \mathbf{R}_d^{1/2} \mathbf{u}_d \right|^2 \right\} = \left\| \mathbf{R}_d^{1/2} \mathbf{a}_b \right\|_2^2$. As such, we have $\left| \mathbf{a}_b^H \mathbf{R}_d^{1/2} \mathbf{u}_d \right| \sim \frac{1}{\sqrt{2}} \left\| \mathbf{R}_d^{1/2} \mathbf{a}_b \right\|_2 X^{1/2}$ where $X \sim \chi_2^2$ is a central chi-squared variable. By the moments of a central chi-square distribution with 2 degrees of freedom,

$$\mathbb{E}\left\{ \left| \mathbf{a}_b^H \mathbf{R}_d^{1/2} \mathbf{u}_d \right| \right\} = \left\| \mathbf{R}_d^{1/2} \mathbf{a}_b \right\|_2 \frac{\sqrt{\pi}}{2}. \quad (21)$$

Hence,

$$\mathbb{E}\{S_2\} = \frac{NA\pi}{2} \sqrt{\beta_d \beta_{br} \beta_{ru}}, \quad (22)$$

where $A = \left\| \mathbf{R}_d^{1/2} \mathbf{a}_b \right\|_2$.

Term 3: Using $|\psi| = 1$ (where ψ is given in Sec. II-B) we have $S_3 = M\beta_{br}\beta_{ru}Y^2$ and expanding Y gives

$$\mathbb{E}\{Y^2\} = \sum_{i=1}^N \mathbb{E}\left\{ \left| \tilde{\mathbf{h}}_{ru,i} \right|^2 \right\} + \sum_{i=1}^N \sum_{\substack{j=1 \\ i \neq j}}^N \mathbb{E}\left\{ \left| \tilde{\mathbf{h}}_{ru,i} \right| \left| \tilde{\mathbf{h}}_{ru,j} \right| \right\}.$$

Using [16, Eq. (16)], each term in the double summation is, $\mathbb{E}\left\{ \left| \tilde{\mathbf{h}}_{ru,i} \right| \left| \tilde{\mathbf{h}}_{ru,j} \right| \right\} = \frac{\pi}{4} \left(1 - |\rho_{ij}|^2 \right)^2 {}_2F_1\left(\frac{3}{2}, \frac{3}{2}; 1; |\rho_{ij}|^2 \right)$, where ${}_2F_1(\cdot)$ is the Gaussian hypergeometric function and $\rho_{ij} = (\mathbf{R}_{ru})_{ij}$. Using this, we have $\mathbb{E}\{Y^2\} = N + F$, where F is given by (7), giving the final result

$$\mathbb{E}\{S_3\} = \beta_{br}\beta_{ru}M(N + F). \quad (23)$$

Combining (20), (22) and (23) completes the derivation.

APPENDIX B

VAR{SNR} DERIVATION IN SEC. III-A

To compute the variance we take the square of (5) giving,

$$\begin{aligned} \text{SNR}^2 &= \left(\beta_d^2 (\mathbf{u}_d^H \mathbf{R}_d \mathbf{u}_d)^2 + 4\beta_d^{3/2} \mathbf{u}_d^H \mathbf{R}_d \mathbf{u}_d \Re \left\{ \alpha \mathbf{u}_d^H \mathbf{R}_d^{1/2} \mathbf{a}_b \right\} \right. \\ &\quad \left. + 2\beta_d M |\alpha|^2 \mathbf{u}_d^H \mathbf{R}_d \mathbf{u}_d + 4\beta_d \Re \left\{ \alpha \mathbf{u}_d^H \mathbf{R}_d^{1/2} \mathbf{a}_b \right\}^2 \right. \\ &\quad \left. + 4\sqrt{\beta_d} M |\alpha|^2 \Re \left\{ \alpha \mathbf{u}_d^H \mathbf{R}_d^{1/2} \mathbf{a}_b \right\} + |\alpha|^4 M^2 \right) \bar{\tau}^2 \\ &\triangleq (T_1 + T_2 + T_3 + T_4 + T_5 + T_6) \bar{\tau}^2. \end{aligned} \quad (24)$$

Terms 1, 3, 4, 5 and 6 can be computed using standard results, the results in [17, Eq. (9)] and the methods given in App. A. The results are,

$$\mathbb{E}\{T_1\} = \beta_d^2 (\text{tr}\{\mathbf{R}_d^2\} + M^2), \quad (25)$$

$$\mathbb{E}\{T_3\} = 2\beta_d \beta_{br} \beta_{ru} M^2 (N + F), \quad (26)$$

$$\mathbb{E}\{T_4\} = 4\beta_d \beta_{br} \beta_{ru} (N + F) \left\| \mathbf{R}_d^{1/2} \mathbf{a}_b \right\|_2^2, \quad (27)$$

$$\mathbb{E}\{T_5\} = 2M \sqrt{\pi} \sqrt{\beta_d} (\beta_{br} \beta_{ru})^{3/2} \left\| \mathbf{R}_d^{1/2} \mathbf{a}_b \right\|_2 \mathbb{E}\{Y^3\}, \quad (28)$$

$$\mathbb{E}\{T_6\} = (M \beta_{br} \beta_{ru})^2 \mathbb{E}\{Y^4\}. \quad (29)$$

The variables Y^3 and Y^4 are the sum of products of magnitudes of 3 and 4 correlated complex Gaussian random variables. To the best of our knowledge the mean of such terms is intractable without the use of multiple infinite summations and special functions. As such we use an approximation based on the gamma distribution to approximate $\mathbb{E}\{Y^3\}$, $\mathbb{E}\{Y^4\}$ (see App. C). Term 2 requires more work and is derived below.

Term 2: Expanding the second term gives,

$$\mathbb{E}\{T_2\} = 4\beta_d^{3/2} \sqrt{\beta_{br} \beta_{ru}} Y \mathbf{u}_d^H \mathbf{R}_d \mathbf{u}_d \left| \mathbf{u}_d^H \mathbf{R}_d^{1/2} \mathbf{a}_b \right|, \quad (30)$$

where Y is defined in Sec. II-B. To find the expectation of (30), we introduce the following variables: Let \mathbf{P} be any orthonormal matrix with first column equal to $\mathbf{p}_1 = \mathbf{R}_d^{1/2} \mathbf{a}_b / \left\| \mathbf{R}_d^{1/2} \mathbf{a}_b \right\|_2^{-1}$. Also let $\mathbf{x} = \mathbf{P}^H \mathbf{u}_d \sim \mathcal{CN}(\mathbf{0}, \mathbf{I})$ and $\mathbf{Q} = \mathbf{P}^H \mathbf{R}_d \mathbf{P}$, then the random component of (30), neglecting Y , can be rewritten as,

$$\mathbf{u}_d^H \mathbf{R}_d \mathbf{u}_d \left| \mathbf{u}_d^H \mathbf{R}_d^{1/2} \mathbf{a}_b \right| = \mathbf{x}^H \mathbf{Q} \mathbf{x} |x_1| \left\| \mathbf{R}_d^{1/2} \mathbf{a}_b \right\|_2,$$

since $\mathbf{P}^H \mathbf{p}_1 = [1, \mathbf{0}_{M-1}^T]^T$. Note that,

$$\begin{aligned} \mathbb{E}\{\mathbf{x}^H \mathbf{Q} \mathbf{x} |x_1|\} &= \mathbb{E}\left\{ \sum_{i=1}^M \sum_{j=1}^M \mathbf{Q}_{ij} x_i^* x_j |x_1| \right\} \\ &= \mathbf{Q}_{11} \mathbb{E}\{|x_1|^3\} + (\text{tr}\{\mathbf{Q}\} - \mathbf{Q}_{11}) \mathbb{E}\{|x_1|\} \\ &= \frac{\sqrt{\pi} \mathbf{a}_b^H \mathbf{R}_d^2 \mathbf{a}_b}{4A^2} + M \frac{\sqrt{\pi}}{2} \end{aligned}$$

since $\mathbb{E}\{|x_1|\} = \sqrt{\pi}/2$, $\mathbb{E}\{|x_1|^3\} = 3\sqrt{\pi}/4$, $\text{tr}\{\mathbf{Q}\} = \text{tr}\{\mathbf{R}_d\} = M$ and $\mathbf{Q}_{11} = \mathbf{p}_1^H \mathbf{R}_d \mathbf{p}_1 = \frac{\mathbf{a}_b^H \mathbf{R}_d^2 \mathbf{a}_b}{\mathbf{a}_b^H \mathbf{R}_d \mathbf{a}_b}$ and A is defined in App. A. Using the above result and the result for $\mathbb{E}\{Y\}$ in App. A, the expectation of (30) is

$$\mathbb{E}\{T_2\} = \beta_d^{3/2} \sqrt{\beta_{br} \beta_{ru}} N B \pi, \quad (31)$$

where $B = M A + \mathbf{a}_b^H \mathbf{R}_d^2 \mathbf{a}_b / 2A$.

Combining (25), (31), (26), (27), (28), (29) for $\mathbb{E}\{\text{SNR}^2\}$ and subtracting $\mathbb{E}\{\text{SNR}\}^2$ completes the derivation.

APPENDIX C

 APPROXIMATIONS FOR $\mathbb{E}\{Y^3\}$ AND $\mathbb{E}\{Y^4\}$

Due to Y being positive, unimodal and the sum of N variables, we propose approximations for $\mathbb{E}\{Y^3\}$ and $\mathbb{E}\{Y^4\}$ using a gamma distribution as an approximation for Y (using the same motivation as in Sec. V-A). From App. A, we know that $\mathbb{E}\{Y\} = N\sqrt{\pi}/2$ and $\mathbb{E}\{Y^2\} = N + F$, where F is defined by (7). Then, the variance of Y is $\text{Var}\{Y\} = N + F - \frac{N^2\pi}{4}$. Using the method of moments, the shape and scale parameters that define the gamma fit for Y are,

$$a = \frac{N^2\pi}{4(N+F) - N^2\pi}, \quad b = \frac{2}{N\sqrt{\pi}} \left(N + F - \frac{N^2\pi}{4} \right),$$

where a and b are the shape and scale parameters respectively. The 3rd and 4th moments of Y are approximated by,

$$\mathbb{E}\{Y^3\} = b^3 a \prod_{k=1}^2 (k+a), \quad \mathbb{E}\{Y^4\} = b^4 a \prod_{k=1}^3 (k+a).$$

Thus we have the results for C_1, C_2 in Sec. III-A.

REFERENCES

- [1] K. Ying *et al.*, "GMD-based hybrid beamforming for large reconfigurable intelligent surface assisted millimeter-wave massive MIMO," *IEEE Access*, vol. 8, pp. 19 530–19 539, 2020.
- [2] Q. Nadeem *et al.*, "Asymptotic max-min SINR analysis of reconfigurable intelligent surface assisted MISO systems," *IEEE Trans. Wireless Commun.*, pp. 1–1, 2020.
- [3] Q. Wu and R. Zhang, "Intelligent reflecting surface enhanced wireless network via joint active and passive beamforming," *IEEE Trans. Wireless Commun.*, vol. 18, no. 11, pp. 5394–5409, 2019.
- [4] H. Yu *et al.*, "Joint design of reconfigurable intelligent surfaces and transmit beamforming under proper and improper Gaussian signaling," *IEEE J. Sel. Areas Commun.*, pp. 1–1, 2020.
- [5] Q. Nadeem *et al.*, "Intelligent reflecting surface-assisted multi-user MISO communication: Channel estimation and beamforming design," *IEEE Open J. of the Commun. Soc.*, vol. 1, pp. 661–680, 2020.
- [6] J. Zhang *et al.*, "Transmitter design for large intelligent surface-assisted MIMO wireless communication with statistical CSI," in *Proc. IEEE ICC Workshops*, 2020, pp. 1–5.
- [7] Q. Nadeem *et al.*, "Opportunistic beamforming using an intelligent reflecting surface without instantaneous CSI," *IEEE Wireless Commun. Lett.*, pp. 1–1, 2020.
- [8] M. M. Zhao *et al.*, "Intelligent reflecting surface enhanced wireless network: Two-timescale beamforming optimization," *IEEE Trans. Wireless Commun.*, pp. 1–1, 2020.
- [9] N. N. Kundu and M. R. McKay, "RIS-Assisted MISO Communication: Optimal Beamformers and Performance Analysis," *arXiv preprint arXiv:2007.08309v2*, 2020.
- [10] A. A. Boulogeorgos and A. Alexiou, "Performance analysis of reconfigurable intelligent surface-assisted wireless systems and comparison with relaying," *IEEE Access*, vol. 8, pp. 94 463–94 483, 2020.
- [11] Q. Tao *et al.*, "Performance analysis of intelligent reflecting surface aided communication systems," *IEEE Commun. Lett.*, pp. 1–1, 2020.
- [12] M. Jung *et al.*, "Asymptotic optimality of reconfigurable intelligent surfaces: Passive beamforming and achievable rate," in *Proc. IEEE ICC*, 2020, pp. 1–6.
- [13] M. Abramowitz and I. A. Stegun, *Handbook of Mathematical Functions with Formulas, Graphs, and Mathematical Tables*. Dover, 1964.
- [14] C. L. Miller *et al.*, "Analytical framework for full-dimensional massive MIMO with ray-based channels," *IEEE J. Sel. Topics Signal Process.*, vol. 13, no. 5, pp. 1181–1195, 2019.
- [15] S. Atapattu *et al.*, "A mixture Gamma distribution to model the SNR of wireless channels," *IEEE Trans. Wireless Commun.*, vol. 10, no. 12, pp. 4193–4203, 2011.
- [16] S. Li *et al.*, "Analysis of analog and digital MRC for distributed and centralized MU-MIMO systems," *IEEE Trans. Veh. Technol.*, vol. 68, no. 2, pp. 1948–1952, 2019.
- [17] H. Tataria *et al.*, "Spatial correlation variability in multiuser systems," in *Proc. IEEE ICC*, 2018, pp. 1–7.